Observations on turbulence dynamics and beam-ion driven modes on the TEXTOR tokamak

C.A. de Meijere[1], S. Coda[1], A. Krämer-Flecken[2], S. Soldatov[2], M. Albergante[1]

[1] *Ecole Polytechnique Fédérale de Lausanne (EPFL), Centre de Recherches en Physique des Plasmas, Association Euratom-Confédération Suisse, CH-1015 Lausanne, Switzerland*

[2] *Institut für Energieforschung - Plasmaphysik, Forschungszentrum Jülich GmbH, Association EURATOM-FZJ, Trilateral Euregio Cluster, 52425 Jülich, Germany*

Introduction

To achieve H-mode the TEXTOR tokamak [1] is operated at weaker than usual toroidal magnetic field ($B_t = 1.3$ T). In both L- and H-mode this leads to quasi periodic bursts of two distinct types of modes (fishbone and Alfvén), both driven unstable by suprathermal beam ions. Although this phenomenology is well known from other experiments [2], it had not yet been documented for the case of TEXTOR. A presentation to this end constitutes the first part of the present paper. We then discuss observations of interaction between the fishbone and the Alfvén modes, and their statistical link to ELMs. Finally, we discuss a third type of mode, unrelated to either the fishbone or the Alfvén modes, which is shown to modulate the amplitude of broad band turbulence in the pedestal during periods leading to ELM crashes.

Observations of beam-ion driven modes

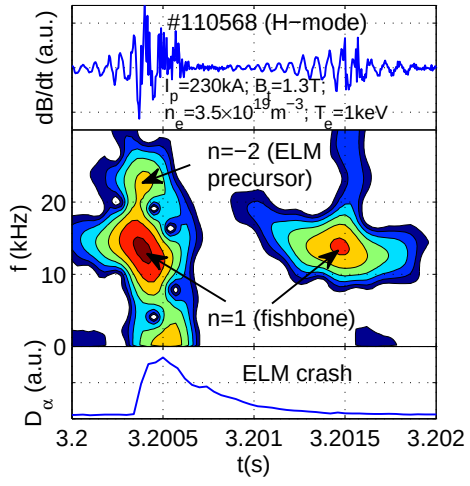

Figure 1: Contours (4 dB interval) of spectral power $\dot{B}_p$; $\Delta t_{\mathrm{win}} = 0.5$ ms.

Figure 1 shows magnetic-probe measurements of the poloidal field fluctuation ($\dot{B}_p(t)$) and the corresponding spectrogram for two consecutive bursts. Such bursts are only seen for $B_t < 1.6$ T and start roughly 20 ms after the neutral beam (1 MW tangential injection of 56 keV deuterium atoms) is switched on. The magnetic spectra during bursts are dominated by a down-chirping $n = 1$ mode, propagating in the ion-diamagnetic drift direction. All this phenomenology matches that of the 'fishbone' mode [3], which is driven by suprathermal beam-ions.

The fishbone is accompanied by several Alfvén modes with frequencies between 100 and 200 kHz in the lab frame. These modes are driven by beam ions, which have parallel velocities up to $v_{\mathrm{b}} = 2 \times 10^6$ m/s, compared to a core Alfvén velocity $v_{\mathrm{A}} = 5 \times 10^6$ m/s. For these experi-

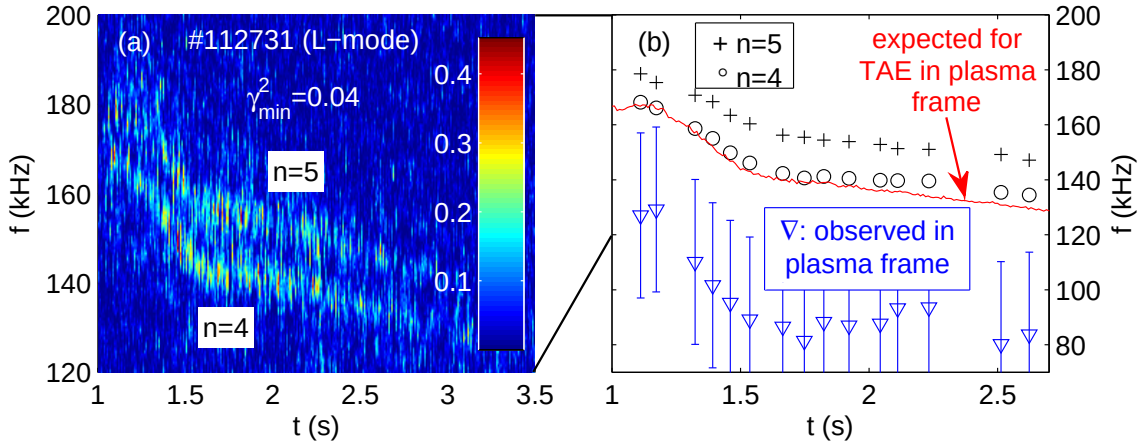

Figure 2: Contours of coherence between phase signals from two reflectometer antennas separated toroidally by 90°; features correspond to Alfvénic modes.

ments the sampling rate of the Mirnov coil signals was insufficient to resolve the Alfvén modes, which have instead been studied using a heterodyne, O-mode reflectometer [4]. This diagnostic features two equatorial antenna arrays, toroidally separated by 90°, and one array viewing the top of the plasma (Fig. 4). The available range of microwave frequencies (28-36 GHz) results in cut-off layers with $r/a > 0.75$ in L-mode and $r/a > 0.9$ in H-mode; the signals were sampled at 1 MHz. During ELMs and L-mode, small-scale density fluctuations strongly scatter the probing microwave beam, so that the signature even of coherent plasma fluctuations is almost totally obscured in the spectral power of the phase signals from the reflectometer. However, the Alfvén (and fishbone) modes are evident as peaks in the *spectral coherence* between phase signals from the various antenna pairs. Figure 2 gives an example for an L-mode discharge in which B_t was ramped down from 1.5-1.3 T on $1.0 < t < 1.6$ s, while n_e increased from $2.7 - 4.0 \times 10^{19}$ m^{-3} on $1.0 < t < 3.5$ s. As expected for Alfvén modes the mode frequencies scale with $B/\sqrt{n_e}$ to within the error bars of the measurements.

The cross-phase spectrum corresponding to Fig. 2 is consistent with the Alfvén modes having toroidal mode numbers $n_1 = 4$ and $n_2 = 5$, propagating in the ion-diamagnetic drift direction. Assuming that the frequency difference between the two observed modes is caused solely by different Doppler shifts we use our tentative estimates of n to calculate the mode frequency in the plasma frame [5], which is shown in Fig. 2b. The obtained frequency is significantly lower than what would be expected for a toroidicity induced Alfvén eigenmode (TAE) driven at $q = 1.5$ [2]. Future attempts to identify these modes, which might be β-induced Alfvén eigenmodes (BAE) [6], should take the high value of normalized plasma-β in these experiments (up to $\beta_N \approx 3$) into account.

A large majority of the fishbones coincide with ELM crashes, like the first one in Fig. 1. In

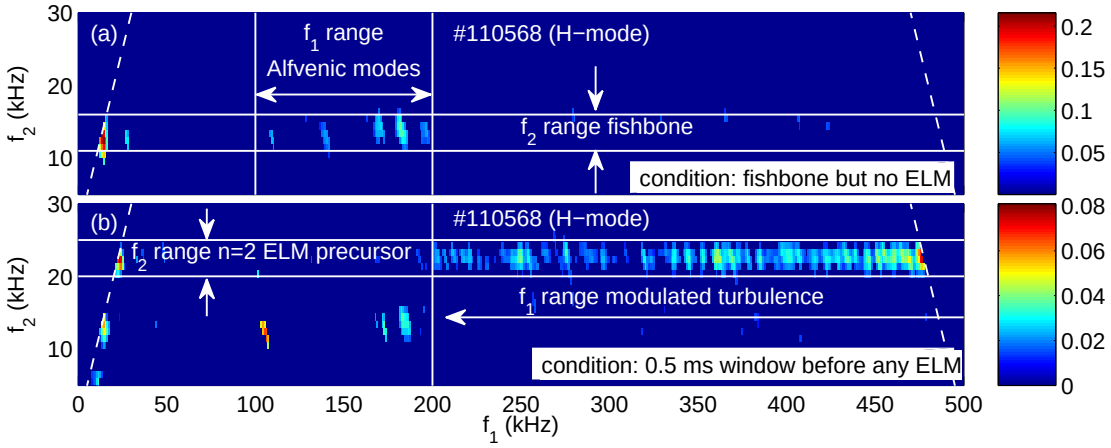

Figure 3: Bispectral coherence of the reflectometer phase signal, averaged over two different conditionally constructed ensembles. Dashed lines indicate the principal domain.

this case the fishbone systematically starts to grow in amplitude tens of μs before the ELM is visible in the D_α signal, so one can speculate that it may actually trigger the ELM crash [3, 7]. However, a minority of the fishbones, like the second one in Fig. 1, clearly do *not* coincide with an ELM. Selecting windows of length 0.5 ms around the latter type of fishbones, we constructed an ensemble of 298 sub-records of a reflectometer phase signal for H-mode discharge 110568. Fig. 3a shows the bispectral coherence, averaged over this ensemble. The spectral features with $100 < f_1 < 200$ khz and $f_2 = 14$ kHz indicate the presence of non-linear interaction between the fishbone and the Alfvén modes [8].

Measurement of turbulence propagation

Between ELMs there are periods of strongly reduced turbulence amplitude, during which the standard deviation of the reflectometer phase signals drops to below 1 radian. Selecting these periods, we construct an ensemble of phase signals from poloidally closely spaced reflectometer antennas (Fig. 4a) and evaluate the cross-spectra. The coherence is low (but significant) and featureless for $f > 200$ kHz, up to the Nyquist frequency of 500 kHz. Let $\Delta\theta_i$ and $\Delta\Psi_i(f)$ denote the angular separation of the detection volumes and the cross-phase, respectively, of antenna combination i. Assuming that the fluctuations obey a single-valued dispersion relation $m(f)$ in the lab-frame (i.e. neglecting turbulent broadening), we have $m(f) = \Delta\Psi_i(f)/\Delta\theta_i$, where m is the poloidal mode number. Figure 4b suggests that broad band fluctuations with $30 < m < 80$ propagate poloidally past the reflectometer, at a group velocity of 26 krad/s in the electron-diamagnetic drift direction.

Turbulence modulation by $n = 2$ ELM precursor mode

In addition to the fishbone, the spectrogram of $\dot{B}_p$ in Fig. 1 shows an $n = 2$ feature at 23 kHz around the time of the ELM crash, which is also visible in the reflectometer phase signals. The

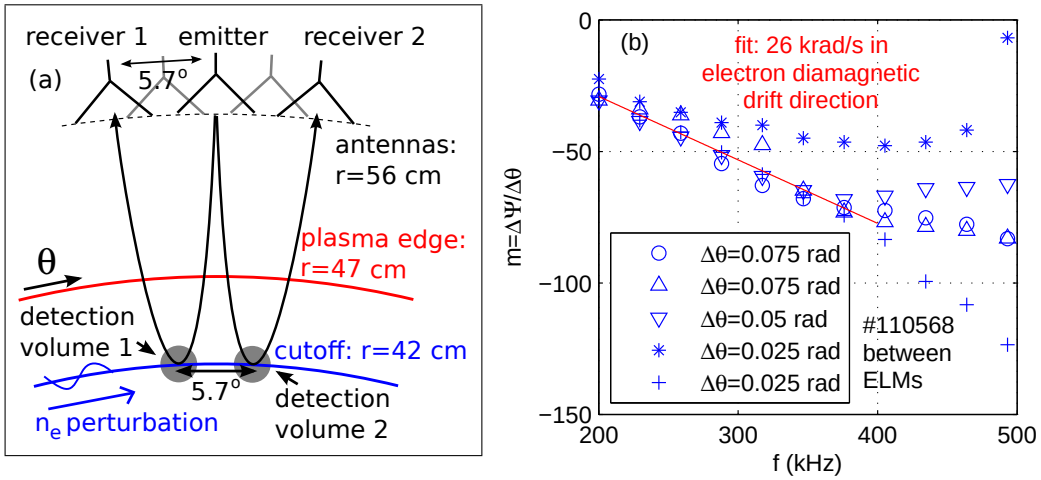

Figure 4: (a) Poloidal section showing one antenna array. (b) Measured dispersion relation of broad band density fluctuations.

mode propagates in the electron-diamagnetic drift direction and poloidal harmonics have $m = 4$ and $m = 5$, giving it a poloidal propagation velocity of roughly 30 krad/s. Since it is only visible in periods of duration 0.5 ms leading up to ELM crashes, we label this mode '$n = 2$ ELM precursor'.

Selecting these 0.5 ms periods before every ELM, we constructed an ensemble of 890 sub-records of the reflectometer phase signal. Figure 3b shows the corresponding averaged bis-pectral coherence, which features a conspicuous ridge for $f_2 = 23$ kHz (corresponding to the $n = 2$ ELM precursor) and $f_1 > 200$ kHz, corresponding to broad-band density fluctuations. The biphase (not shown) is constant along this ridge. These observations strongly suggest that the $n = 2$ ELM precursor modulates the amplitude of turbulent electron density fluctuations in the H-mode pedestal, whose poloidal group velocity matches that of the $n = 2$ mode.

This work was supported in part by the Swiss National Science Foundation.

References

[1] B. Unterberg et al, J. Nucl. Mater. **390-391** (2009) 351

[2] W.W. Heidbrink, Phys. Plasmas **15** (2008) 055501-1

[3] T. Kass et al, Nucl. Fusion **38** (1998) 807

[4] A. Krämer-Flecken et al, Plasma Phys. Controlled Fusion **51** (2009) 015001

[5] E.J. Strait et al, Plasma Phys. Controlled Fusion **36** (1995) 1211

[6] W.W. Heidbrink et al, Phys. Rev. Lett. **71** (1993) 855

[7] G. Matsunaga et al, Proceedings of the 23rd IAEA Fusion Energy Conference (2010) EXS/5-3

[8] N.A. Crocker et al, Phys. Rev. Lett. **97** (2006) 045002